

Aerodynamic Shape Optimization for Aircraft Design

Antony Jameson

*Department of Aeronautics and Astronautics
Stanford University, Stanford, CA*

6th World Congress of Computational Mechanics
Beijing, China
September 6-10, 2004

✎ Aerodynamic Design Tradeoffs

A good first estimate of performance is provided by the Breguet range equation:

$$Range = \frac{VL}{D} \frac{1}{SFC} \log \frac{W_0 + W_f}{W_0}. \quad (1)$$

Here V is the speed, L/D is the lift to drag ratio, SFC is the specific fuel consumption of the engines, W_0 is the loading weight (empty weight + payload + fuel resourced), and W_f is the weight of fuel burnt.

Equation (1) displays the multidisciplinary nature of design.

A light structure is needed to reduce W_0 . SFC is the province of the engine manufacturers. The aerodynamic designer should try to maximize $\frac{VL}{D}$. This means the cruising speed V should be increased until the onset of drag rise at a Mach Number $M = \frac{V}{C} \sim .85$. But the designer must also consider the impact of shape modifications in structure weight.

✎ Aerodynamic Design Tradeoffs

The drag coefficient can be split into an approximate fixed component C_{D_0} , and the induced drag due to lift.

$$C_D = C_{D_0} + \frac{C_L^2}{\pi \varepsilon AR} \quad (2)$$

where AR is the aspect ratio, and ε is an efficiency factor close to unity. C_{D_0} includes contributions such as friction and form drag. It can be seen from this equation that L/D is maximized by flying at a lift coefficient such that the two terms are equal, so that the induced drag is half the total drag. Moreover, the actual drag due to lift

$$D_v = \frac{2L^2}{\pi \varepsilon \rho V^2 b^2}$$

varies inversely with the square of the span b . Thus there is a direct conflict between reducing the drag by increasing the span and reducing the structure weight by decreasing it.

👉 Overall Design Process

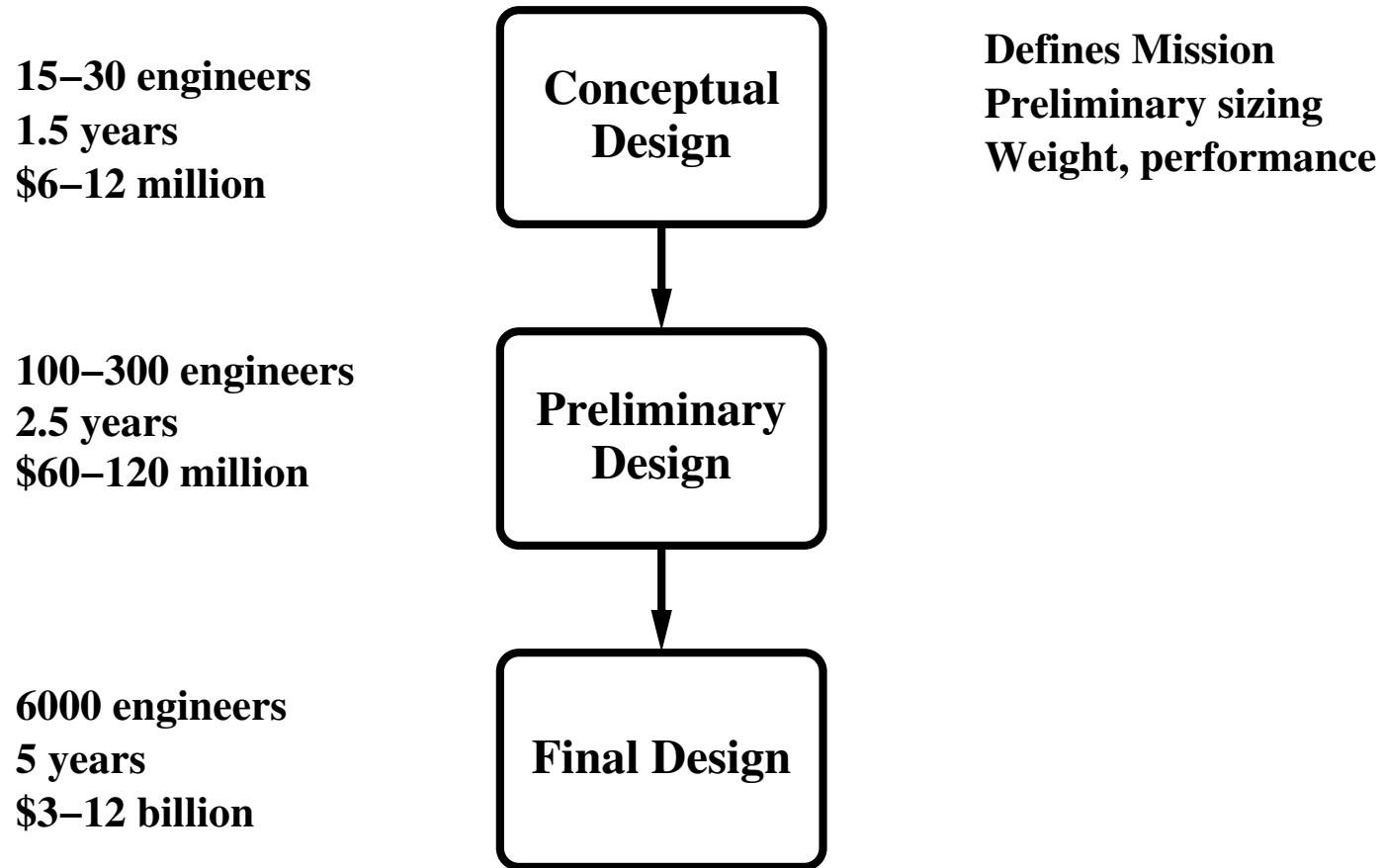
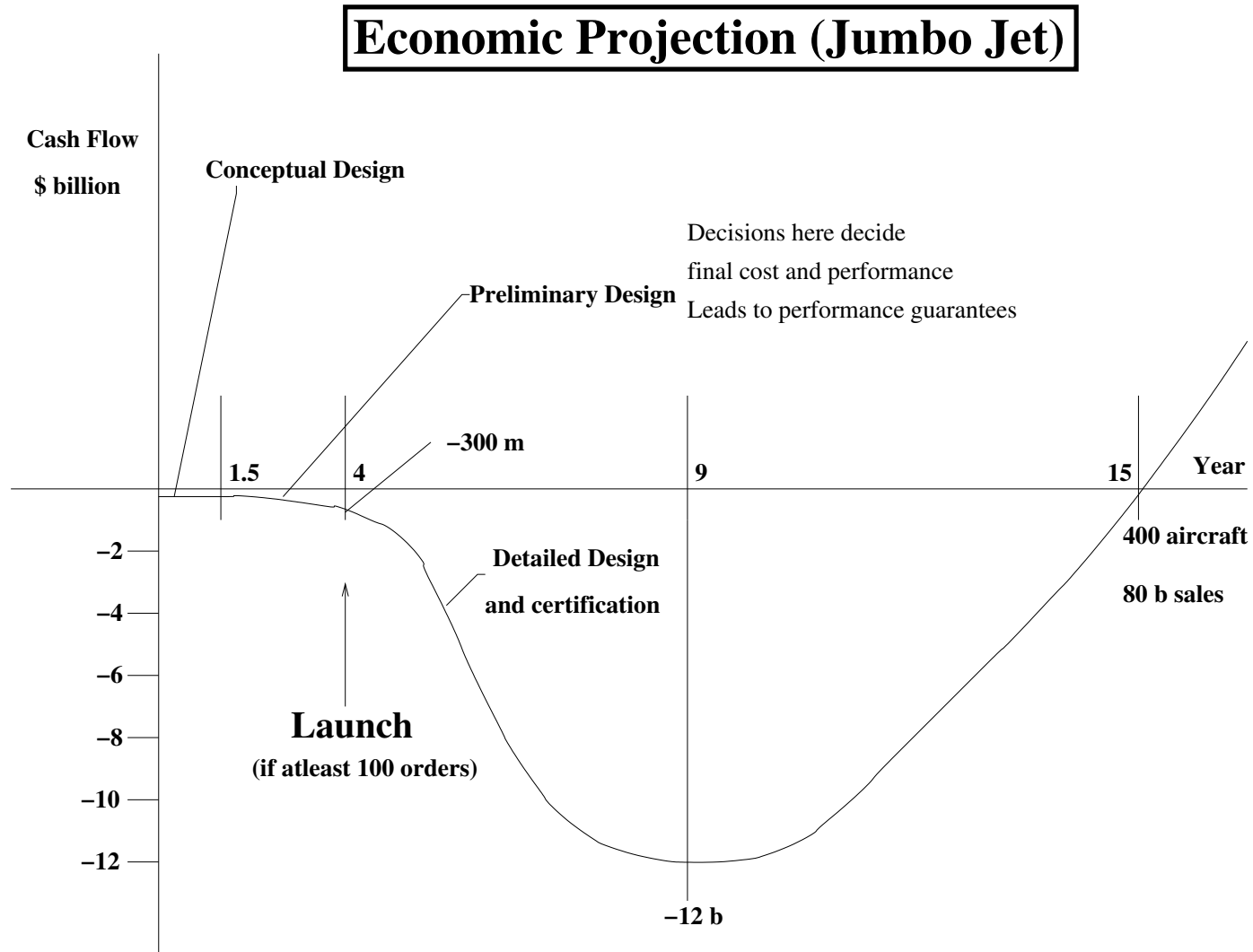


Figure 1: The Overall Design Process

👉 Cash flow



Aerodynamic Design Process

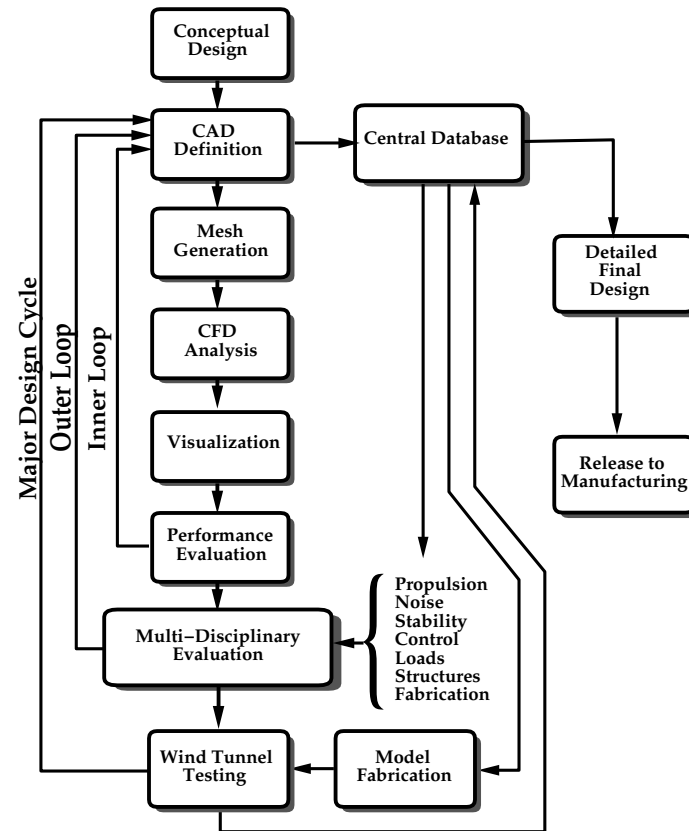


Figure 2: The Aerodynamic Design Process

Effective Simulation



Simulation-based Design

☞ Automatic Design Based on Control Theory

- Regard the wing as a device to generate lift (with minimum drag) by controlling the flow
- Apply theory of optimal control of systems governed by PDEs (Lions) with boundary control (the wing shape)
- Merge control theory and CFD

☞ Automatic Shape Design via Control Theory

- Apply the theory of control of partial differential equations (of the flow) by boundary control (the shape)
- Find the Frechet derivative (infinite dimensional gradient) of a cost function (performance measure) with respect to the shape by solving the adjoint equation in addition to the flow equation
- Modify the shape in the sense defined by the smoothed gradient
- Repeat until the performance value approaches an optimum

✎ Aerodynamic Shape Optimization: Gradient Calculation

For the class of aerodynamic optimization problems under consideration, the design space is essentially infinitely dimensional. Suppose that the performance of a system design can be measured by a cost function I which depends on a function $\mathcal{F}(x)$ that describes the shape, where under a variation of the design $\delta\mathcal{F}(x)$, the variation of the cost is δI . Now suppose that δI can be expressed to first order as

$$\delta I = \int \mathcal{G}(x) \delta\mathcal{F}(x) dx$$

where $\mathcal{G}(x)$ is the gradient. Then by setting

$$\delta\mathcal{F}(x) = -\lambda\mathcal{G}(x)$$

one obtains an improvement

$$\delta I = -\lambda \int \mathcal{G}^2(x) dx$$

unless $\mathcal{G}(x) = 0$. Thus the vanishing of the gradient is a necessary condition for a local minimum.

✎ Aerodynamic Shape Optimization: Gradient Calculation

Computing the gradient of a cost function for a complex system can be a numerically intensive task, especially if the number of design parameters is large and the cost function is an expensive evaluation. The simplest approach to optimization is to define the geometry through a set of design parameters, which may, for example, be the weights α_i applied to a set of shape functions $\mathcal{B}_i(x)$ so that the shape is represented as

$$\mathcal{F}(x) = \sum \alpha_i \mathcal{B}_i(x).$$

Then a cost function I is selected which might be the drag coefficient or the lift to drag ratio; I is regarded as a function of the parameters α_i . The sensitivities $\frac{\partial I}{\partial \alpha_i}$ may now be estimated by making a small variation $\delta \alpha_i$ in each design parameter in turn and recalculating the flow to obtain the change in I . Then

$$\frac{\partial I}{\partial \alpha_i} \approx \frac{I(\alpha_i + \delta \alpha_i) - I(\alpha_i)}{\delta \alpha_i}.$$

👉 Symbolic Development of the Adjoint Method

Let I be the **cost** (or **objective**) function

$$I = I(w, \mathcal{F})$$

where

w = flow field variables

\mathcal{F} = grid variables

The **first variation** of the cost function is

$$\delta I = \frac{\partial I^T}{\partial w} \delta w + \frac{\partial I^T}{\partial \mathcal{F}} \delta \mathcal{F}$$

The **flow field equation** and its **first variation** are

$$R(w, \mathcal{F}) = 0$$

$$\delta R = 0 = \left[\frac{\partial R}{\partial w} \right] \delta w + \left[\frac{\partial R}{\partial \mathcal{F}} \right] \delta \mathcal{F}$$

👉 Symbolic Development of the Adjoint Method (cont.)

Introducing a **Lagrange Multiplier**, ψ , and using the **flow field equation** as a **constraint**

$$\begin{aligned}\delta I &= \frac{\partial I^T}{\partial w} \delta w + \frac{\partial I^T}{\partial \mathcal{F}} \delta \mathcal{F} - \psi^T \left\{ \left[\frac{\partial R}{\partial w} \right] \delta w + \left[\frac{\partial R}{\partial \mathcal{F}} \right] \delta \mathcal{F} \right\} \\ &= \left\{ \frac{\partial I^T}{\partial w} - \psi^T \left[\frac{\partial R}{\partial w} \right] \right\} \delta w + \left\{ \frac{\partial I^T}{\partial \mathcal{F}} - \psi^T \left[\frac{\partial R}{\partial \mathcal{F}} \right] \right\} \delta \mathcal{F}\end{aligned}$$

By choosing ψ such that it satisfies the **adjoint equation**

$$\left[\frac{\partial R}{\partial w} \right]^T \psi = \frac{\partial I}{\partial w},$$

we have

$$\delta I = \left\{ \frac{\partial I^T}{\partial \mathcal{F}} - \psi^T \left[\frac{\partial R}{\partial \mathcal{F}} \right] \right\} \delta \mathcal{F}$$

This reduces the **gradient** calculation for an arbitrarily large number of design variables at a **single design point** to

👉 **One Flow Solution** + **One Adjoint Solution**

☞ Design using the Euler Equations

The three-dimensional Euler equations may be written as

$$\frac{\partial w}{\partial t} + \frac{\partial f_i}{\partial x_i} = 0 \quad \text{in } D, \quad (3)$$

where

$$w = \begin{Bmatrix} \rho \\ \rho u_1 \\ \rho u_2 \\ \rho u_3 \\ \rho E \end{Bmatrix}, \quad f_i = \begin{Bmatrix} \rho u_i \\ \rho u_i u_1 + p \delta_{i1} \\ \rho u_i u_2 + p \delta_{i2} \\ \rho u_i u_3 + p \delta_{i3} \\ \rho u_i H \end{Bmatrix} \quad (4)$$

and δ_{ij} is the Kronecker delta function. Also,

$$p = (\gamma - 1) \rho \left\{ E - \frac{1}{2} (u_i^2) \right\}, \quad (5)$$

and

$$\rho H = \rho E + p \quad (6)$$

where γ is the ratio of the specific heats.

👉 Design using the Euler Equations

In order to simplify the derivation of the adjoint equations, we map the solution to a fixed computational domain with coordinates ξ_1, ξ_2, ξ_3 where

$$K_{ij} = \left[\frac{\partial x_i}{\partial \xi_j} \right], \quad J = \det(K), \quad K_{ij}^{-1} = \left[\frac{\partial \xi_i}{\partial x_j} \right],$$

and

$$S = JK^{-1}.$$

The elements of S are the cofactors of K , and in a finite volume discretization they are just the face areas of the computational cells projected in the $x_1, x_2,$ and x_3 directions. Using the permutation tensor ϵ_{ijk} we can express the elements of S as

$$S_{ij} = \frac{1}{2} \epsilon_{jppq} \epsilon_{irs} \frac{\partial x_p}{\partial \xi_r} \frac{\partial x_q}{\partial \xi_s}. \quad (7)$$

👉 Design using the Euler Equations

Then

$$\begin{aligned}\frac{\partial}{\partial \xi_i} S_{ij} &= \frac{1}{2} \epsilon_{j p q} \epsilon_{i r s} \left(\frac{\partial^2 x_p}{\partial \xi_r \partial \xi_i} \frac{\partial x_q}{\partial \xi_s} + \frac{\partial x_p}{\partial \xi_r} \frac{\partial^2 x_q}{\partial \xi_s \partial \xi_i} \right) \\ &= 0.\end{aligned}\tag{8}$$

Also in the subsequent analysis of the effect of a shape variation it is useful to note that

$$\begin{aligned}S_{1j} &= \epsilon_{j p q} \frac{\partial x_p}{\partial \xi_2} \frac{\partial x_q}{\partial \xi_3}, \\ S_{2j} &= \epsilon_{j p q} \frac{\partial x_p}{\partial \xi_3} \frac{\partial x_q}{\partial \xi_1}, \\ S_{3j} &= \epsilon_{j p q} \frac{\partial x_p}{\partial \xi_1} \frac{\partial x_q}{\partial \xi_2}.\end{aligned}\tag{9}$$

👉 Design using the Euler Equations

Now, multiplying equation(3) by J and applying the chain rule,

$$J \frac{\partial w}{\partial t} + R(w) = 0 \quad (10)$$

where

$$R(w) = S_{ij} \frac{\partial f_j}{\partial \xi_i} = \frac{\partial}{\partial \xi_i} (S_{ij} f_j), \quad (11)$$

using (8). We can write the transformed fluxes in terms of the scaled contravariant velocity components

$$U_i = S_{ij} u_j$$

as

$$F_i = S_{ij} f_j = \begin{bmatrix} \rho U_i \\ \rho U_i u_1 + S_{i1} p \\ \rho U_i u_2 + S_{i2} p \\ \rho U_i u_3 + S_{i3} p \\ \rho U_i H \end{bmatrix}.$$

👉 Design using the Euler Equations

For simplicity, it will be assumed that the portion of the boundary that undergoes shape modifications is restricted to the coordinate surface $\xi_2 = 0$. Then equations for the variation of the cost function and the adjoint boundary conditions may be simplified by incorporating the conditions

$$n_1 = n_3 = 0, \quad n_2 = 1, \quad d\mathcal{B}_\xi = d\xi_1 d\xi_3,$$

so that only the variation δF_2 needs to be considered at the wall boundary. The condition that there is no flow through the wall boundary at $\xi_2 = 0$ is equivalent to

$$U_2 = 0, \quad \text{so that} \quad \delta U_2 = 0$$

when the boundary shape is modified. Consequently the variation of the inviscid flux at the boundary reduces to

$$\delta F_2 = \delta p \begin{Bmatrix} 0 \\ S_{21} \\ S_{22} \\ S_{23} \\ 0 \end{Bmatrix} + p \begin{Bmatrix} 0 \\ \delta S_{21} \\ \delta S_{22} \\ \delta S_{23} \\ 0 \end{Bmatrix}. \quad (12)$$

👉 Design using the Euler Equations

In order to design a shape which will lead to a desired pressure distribution, a natural choice is to set

$$I = \frac{1}{2} \int_{\mathcal{B}} (p - p_d)^2 dS$$

where p_d is the desired surface pressure, and the integral is evaluated over the actual surface area. In the computational domain this is transformed to

$$I = \frac{1}{2} \iint_{\mathcal{B}_w} (p - p_d)^2 |S_2| d\xi_1 d\xi_3,$$

where the quantity

$$|S_2| = \sqrt{S_{2j} S_{2j}}$$

denotes the face area corresponding to a unit element of face area in the computational domain.

👉 Design using the Euler Equations

In the computational domain the adjoint equation assumes the form

$$C_i^T \frac{\partial \psi}{\partial \xi_i} = 0 \quad (13)$$

where

$$C_i = S_{ij} \frac{\partial f_j}{\partial w}.$$

To cancel the dependence of the boundary integral on δp , the adjoint boundary condition reduces to

$$\psi_j n_j = p - p_d \quad (14)$$

where n_j are the components of the surface normal

$$n_j = \frac{S_{2j}}{|S_2|}.$$

👉 Design using the Euler Equations

This amounts to a transpiration boundary condition on the co-state variables corresponding to the momentum components. Note that it imposes no restriction on the tangential component of ψ at the boundary.

We find finally that

$$\begin{aligned} \delta I = & - \int_{\mathcal{D}} \frac{\partial \psi^T}{\partial \xi_i} \delta S_{ij} f_j d\mathcal{D} \\ & - \iint_{B_W} (\delta S_{21} \psi_2 + \delta S_{22} \psi_3 + \delta S_{23} \psi_4) p d\xi_1 d\xi_3. \end{aligned} \quad (15)$$

Here the expression for the cost variation depends on the **mesh variations throughout the domain which appear in the field integral**. However, the **true gradient** for a shape variation should not depend on the way in which the mesh is deformed, but **only on the true flow solution**. In the next section we show how the field integral can be eliminated to produce a reduced gradient formula which depends only on the boundary movement.

👉 The Reduced Gradient Formulation

Consider the case of a mesh variation with a fixed boundary. Then,

$$\delta I = 0$$

but there is a variation in the transformed flux,

$$\delta F_i = C_i \delta w + \delta S_{ij} f_j.$$

Here the true solution is unchanged. Thus, the variation δw is due to the mesh movement δx at each mesh point. Therefore

$$\delta w = \nabla w \cdot \delta x = \frac{\partial w}{\partial x_j} \delta x_j (= \delta w^*)$$

and since

$$\frac{\partial}{\partial \xi_i} \delta F_i = 0,$$

it follows that

$$\frac{\partial}{\partial \xi_i} (\delta S_{ij} f_j) = -\frac{\partial}{\partial \xi_i} (C_i \delta w^*). \quad (16)$$

It has been verified by Jameson and Kim* that this relation holds in the general case with boundary movement.

* *Reduction of the Adjoint Gradient Formula in the Continuous Limit*, A. Jameson and S. Kim, 41st AIAA Aerospace Sciences Meeting & Exhibit, AIAA Paper 2003-0040, Reno, NV, January 6-9, 2003.

👉 The Reduced Gradient Formulation

Now

$$\begin{aligned}\int_{\mathcal{D}} \phi^T \delta R d\mathcal{D} &= \int_{\mathcal{D}} \phi^T \frac{\partial}{\partial \xi_i} C_i (\delta w - \delta w^*) d\mathcal{D} \\ &= \int_{\mathcal{B}} \phi^T C_i (\delta w - \delta w^*) d\mathcal{B} \\ &\quad - \int_{\mathcal{D}} \frac{\partial \phi^T}{\partial \xi_i} C_i (\delta w - \delta w^*) d\mathcal{D}.\end{aligned}\tag{17}$$

Here on the wall boundary

$$C_2 \delta w = \delta F_2 - \delta S_{2j} f_j.\tag{18}$$

Thus, by choosing ϕ to satisfy the adjoint equation and the adjoint boundary condition, we reduce the cost variation to a boundary integral which depends only on the surface displacement:

$$\begin{aligned}\delta I &= \int_{\mathcal{B}_W} \psi^T (\delta S_{2j} f_j + C_2 \delta w^*) d\xi_1 d\xi_3 \\ &\quad - \iint_{\mathcal{B}_W} (\delta S_{21} \psi_2 + \delta S_{22} \psi_3 + \delta S_{23} \psi_4) p d\xi_1 d\xi_3.\end{aligned}\tag{19}$$

👉 The Need for a Sobolev Inner Product in the Definition of the Gradient

Another key issue for successful implementation of the continuous adjoint method is the choice of an appropriate inner product for the definition of the gradient. It turns out that there is an enormous benefit from the use of a modified Sobolev gradient, which enables the generation of a sequence of smooth shapes. This can be illustrated by considering the simplest case of a problem in the calculus of variations.

Suppose that we wish to find the path $y(x)$ which minimizes

$$I = \int_a^b F(y, y') dx$$

with fixed end points $y(a)$ and $y(b)$. Under a variation $\delta y(x)$,

$$\begin{aligned} \delta I &= \int_a^b \left(\frac{\partial F}{\partial y} \delta y + \frac{\partial F}{\partial y'} \delta y' \right) dx \\ &= \int_a^b \left(\frac{\partial F}{\partial y} - \frac{d}{dx} \frac{\partial F}{\partial y'} \right) \delta y dx \end{aligned}$$

☞ The Need for a Sobolev Inner Product in the Definition of the Gradient

Thus defining the gradient as

$$g = \frac{\partial F}{\partial y} - \frac{d}{dx} \frac{\partial F}{\partial y'}$$

and the inner product as

$$(u, v) = \int_a^b uv dx$$

we find that

$$\delta I = (g, \delta y).$$

If we now set

$$\delta y = -\lambda g, \quad \lambda > 0$$

we obtain a improvement

$$\delta I = -\lambda (g, g) \leq 0$$

unless $g = 0$, the necessary condition for a minimum.

☞ The Need for a Sobolev Inner Product in the Definition of the Gradient

Note that g is a function of y, y', y'' ,

$$g = g(y, y', y'')$$

In the well known case of the Brachistrone problem, for example, which calls for the determination of the path of quickest descent between two laterally separated points when a particle falls under gravity,

$$F(y, y') = \sqrt{\frac{1 + y'^2}{y}}$$

and

$$g = -\frac{1 + y'^2 + 2yy''}{2(y(1 + y'^2))^{3/2}}$$

It can be seen that each step

$$y^{n+1} = y^n - \lambda^n g^n$$

reduces the smoothness of y by two classes. Thus the computed trajectory becomes less and less smooth, leading to instability.

👉 The Need for a Sobolev Inner Product in the Definition of the Gradient

In order to prevent this we can introduce a weighted Sobolev inner product

$$\langle u, v \rangle = \int (uv + \epsilon u'v') dx$$

where ϵ is a parameter that controls the weight of the derivatives. We now define a gradient \bar{g} such that

$$\delta I = \langle \bar{g}, \delta y \rangle$$

Then we have

$$\begin{aligned} \delta I &= \int (\bar{g} \delta y + \epsilon \bar{g}' \delta y') dx \\ &= \int \left(\bar{g} - \frac{\partial}{\partial x} \epsilon \frac{\partial \bar{g}}{\partial x} \right) \delta y dx \\ &= (g, \delta y) \end{aligned}$$

where

$$\bar{g} - \frac{\partial}{\partial x} \epsilon \frac{\partial \bar{g}}{\partial x} = g$$

and $\bar{g} = 0$ at the end points. Thus \bar{g} can be obtained from g by a smoothing equation. Now the step

$$y^{n+1} = y^n - \lambda^n \bar{g}^n$$

gives an improvement

$$\delta I = -\lambda^n \langle \bar{g}^n, \bar{g}^n \rangle$$

but y^{n+1} has the same smoothness as y^n , resulting in a stable process.

👉 Outline of the Design Process

The design procedure can finally be summarized as follows:

1. Solve the flow equations for ρ , u_1 , u_2 , u_3 , p .
2. Solve the adjoint equations for ψ subject to appropriate boundary conditions.
3. Evaluate \mathcal{G} and calculate the corresponding Sobolev gradient $\bar{\mathcal{G}}$.
4. Project $\bar{\mathcal{G}}$ into an allowable subspace that satisfies any geometric constraints.
5. Update the shape based on the direction of steepest descent.
6. Return to 1 until convergence is reached.

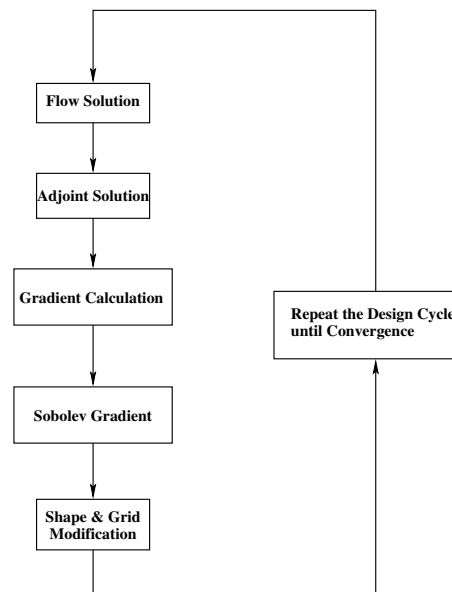


Figure 3: Design cycle

☞ Computational Costs*

Cost of Search Algorithm

Steepest Descent	$\mathcal{O}(N^2)$ steps
Quasi-Newton	$\mathcal{O}(N)$ steps
Smoothed Gradient	$\mathcal{O}(K)$ steps
(Note: K is independent of N)	

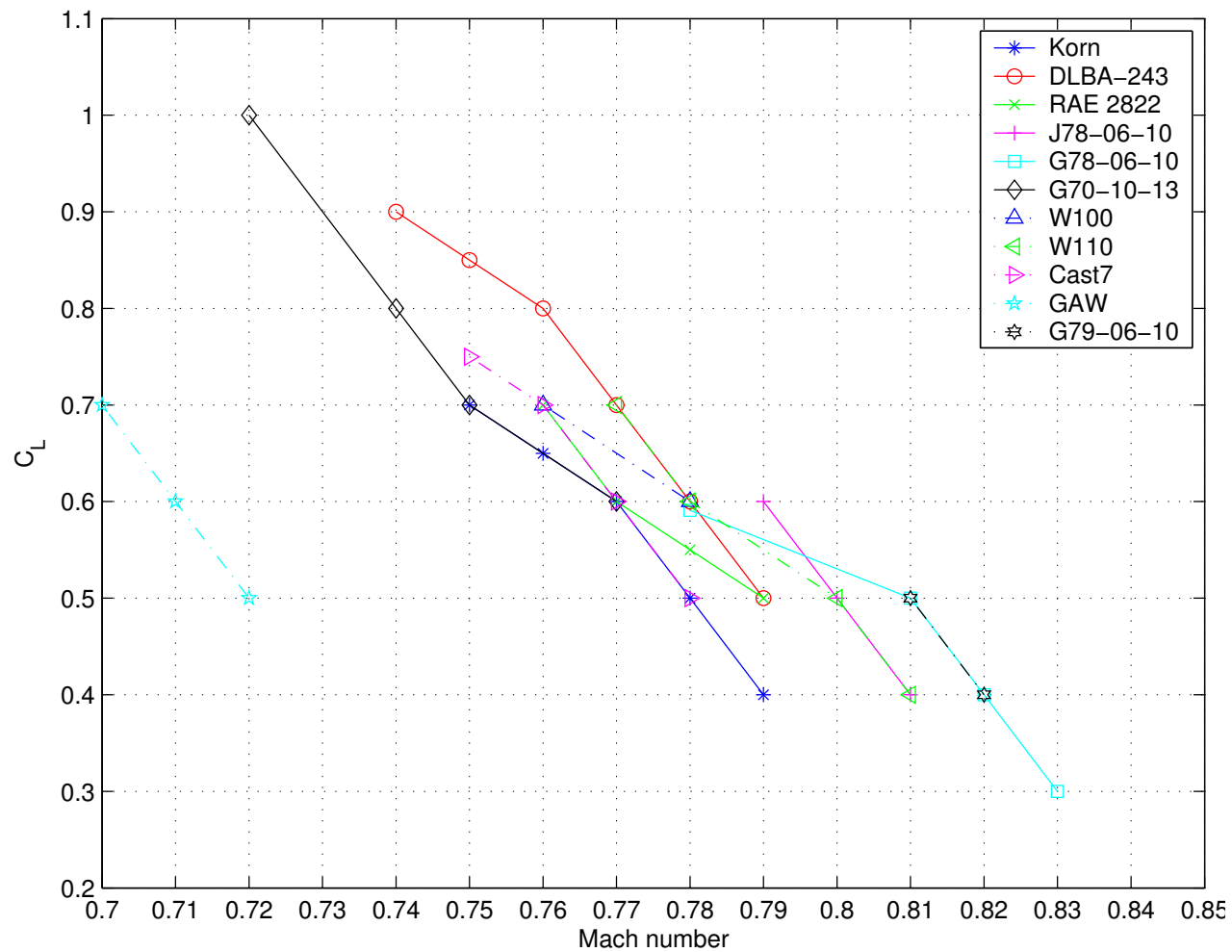
Total Computational Cost of Design

Finite Difference Gradients	
+ Steepest Descent	$\mathcal{O}(N^3)$
Finite Difference Gradients	
+ Quasi-Newton Search	$\mathcal{O}(N^2)$
Adjoint Gradients	
+ Quasi-Newton Search	$\mathcal{O}(N)$
Adjoint Gradients	
+ Smoothed Gradient Search	$\mathcal{O}(K)$
(Note: K is independent of N)	

* *Studies of Alternative Numerical Optimization Methods Applied to the Brachistrone Problem*, A. Jameson and J. Vassberg, Computational Fluid Dynamics, Journal, Vol. 9, No.3, Oct. 2000, pp. 281-296

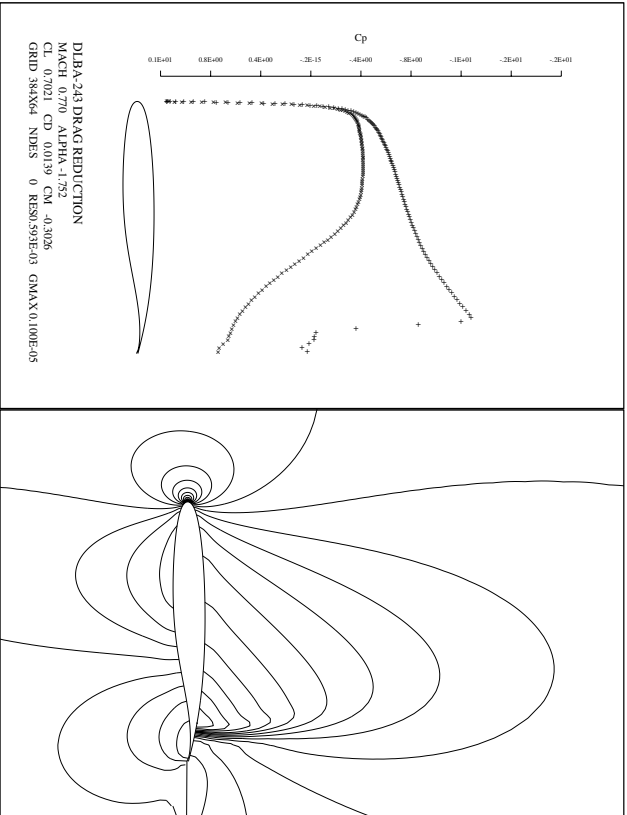
Two dimensional studies of transonic airfoil design

Attainable shock-free solutions for various shape optimized airfoils

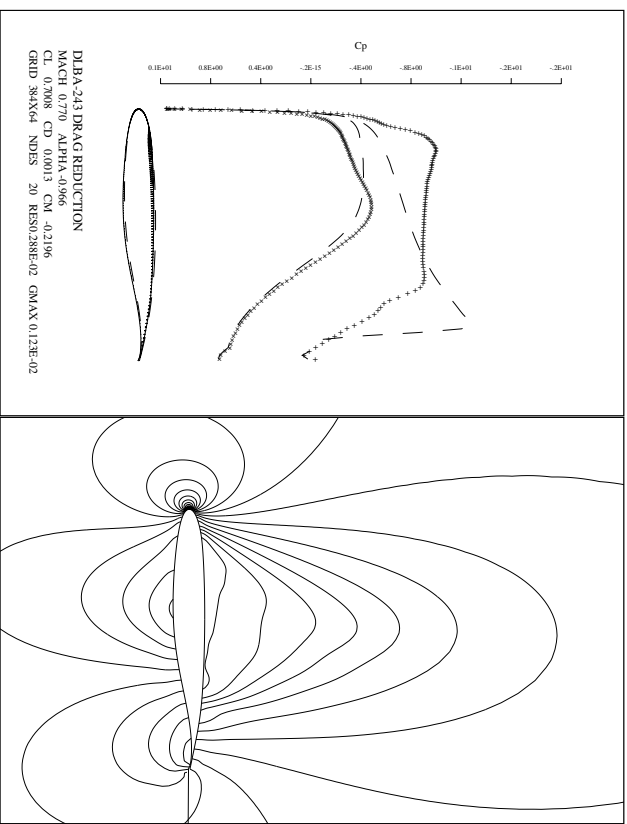




Pressure distribution and Mach contours for the DLBA-243 airfoil

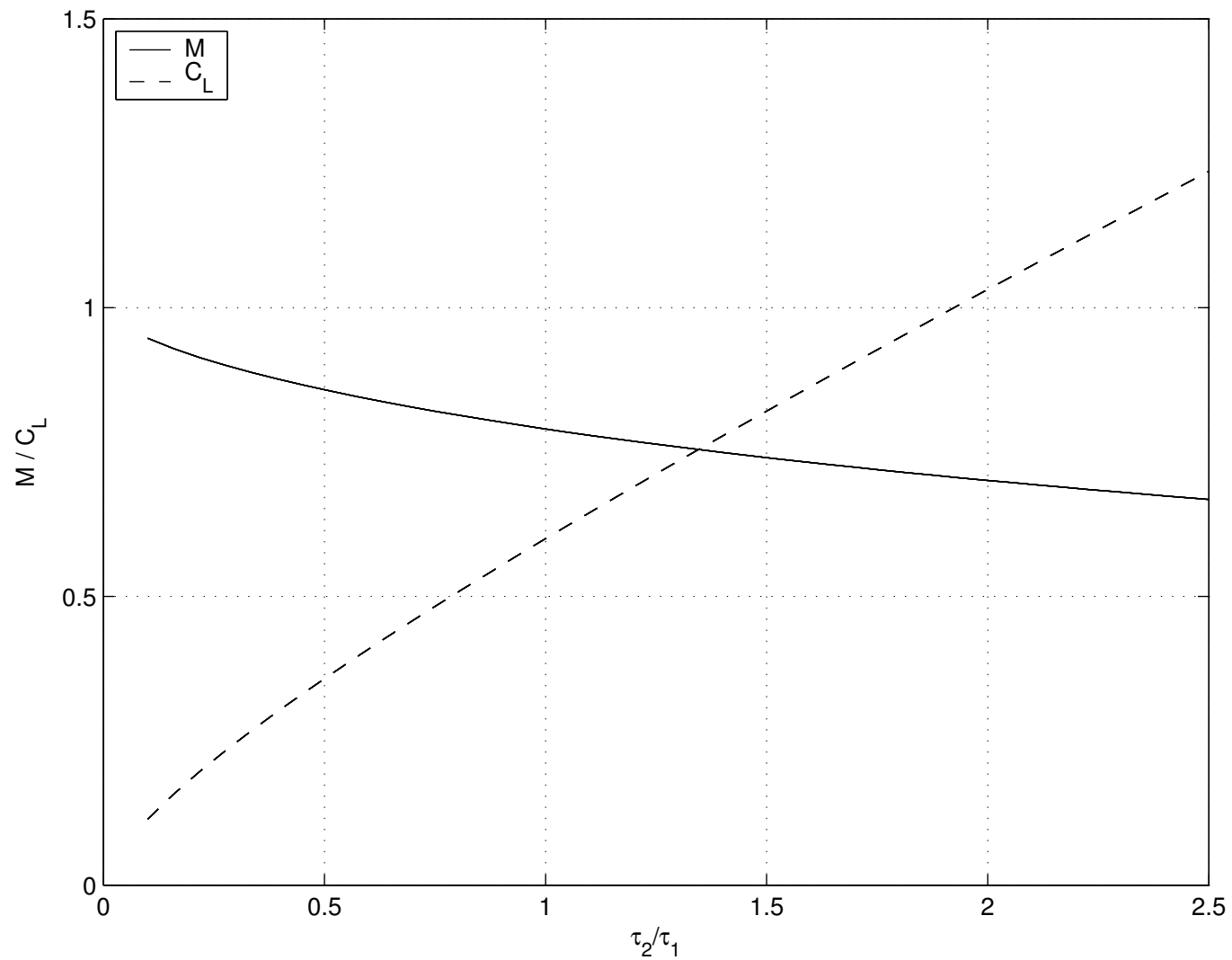


Before the redesign



After the redesign

👉 **Transonic similarity rule: M and C_L scale with thickness ratio**



☞ Planform and Aero-Structural Optimization

The shape changes in the section needed to improve the transonic wing design are quite small. However, in order to obtain a true optimum design larger scale changes such as changes in the wing planform (sweepback, span, chord, and taper) should be considered. Because these directly affect the structure weight, a meaningful result can only be obtained by considering a cost function that takes account of both the aerodynamic characteristics and the weight.

Consider a cost function is defined as

$$I = \alpha_1 C_D + \alpha_2 \frac{1}{2} \int_{\mathcal{B}} (p - p_d)^2 dS + \alpha_3 C_W$$

Maximizing the **range** of an **aircraft** provides a guide to the values for α_1 and α_3 .

☞ Choice of Weighting Constants

The **simplified Breguet range equation** can be expressed as

$$R = \frac{V}{C} \frac{L}{D} \log \frac{W_1}{W_2}$$

where W_2 is the empty weight of the aircraft.

With fixed $\frac{V}{C}$, W_1 , and L , the variation of R can be stated as

$$\begin{aligned} \delta R &= \frac{V}{C} \left(\delta \left(\frac{L}{D} \right) \log \frac{W_1}{W_2} + \frac{L}{D} \delta \left(\log \frac{W_1}{W_2} \right) \right) \\ &= \frac{V}{C} \left(-\frac{\delta D}{D} \frac{L}{D} \log \frac{W_1}{W_2} - \frac{L}{D} \frac{\delta W_2}{W_2} \right) \\ &= -\frac{V}{C} \frac{L}{D} \log \frac{W_1}{W_2} \left(\frac{\delta D}{D} + \frac{1}{\log \frac{W_1}{W_2}} \frac{\delta W_2}{W_2} \right) \end{aligned}$$

Then,

$$\begin{aligned} \frac{\delta R}{R} &= - \left(\frac{\delta C_D}{C_D} + \frac{1}{\log \frac{W_1}{W_2}} \frac{\delta W_2}{W_2} \right) \\ &= - \left(\frac{\delta C_D}{C_D} + \frac{1}{\log \frac{C_{W_1}}{C_{W_2}}} \frac{\delta C_{W_2}}{C_{W_2}} \right). \end{aligned}$$

☞ Choice of Weighting Constants (cont.)

Therefore **minimizing**

$$I = C_D + \alpha C_W,$$

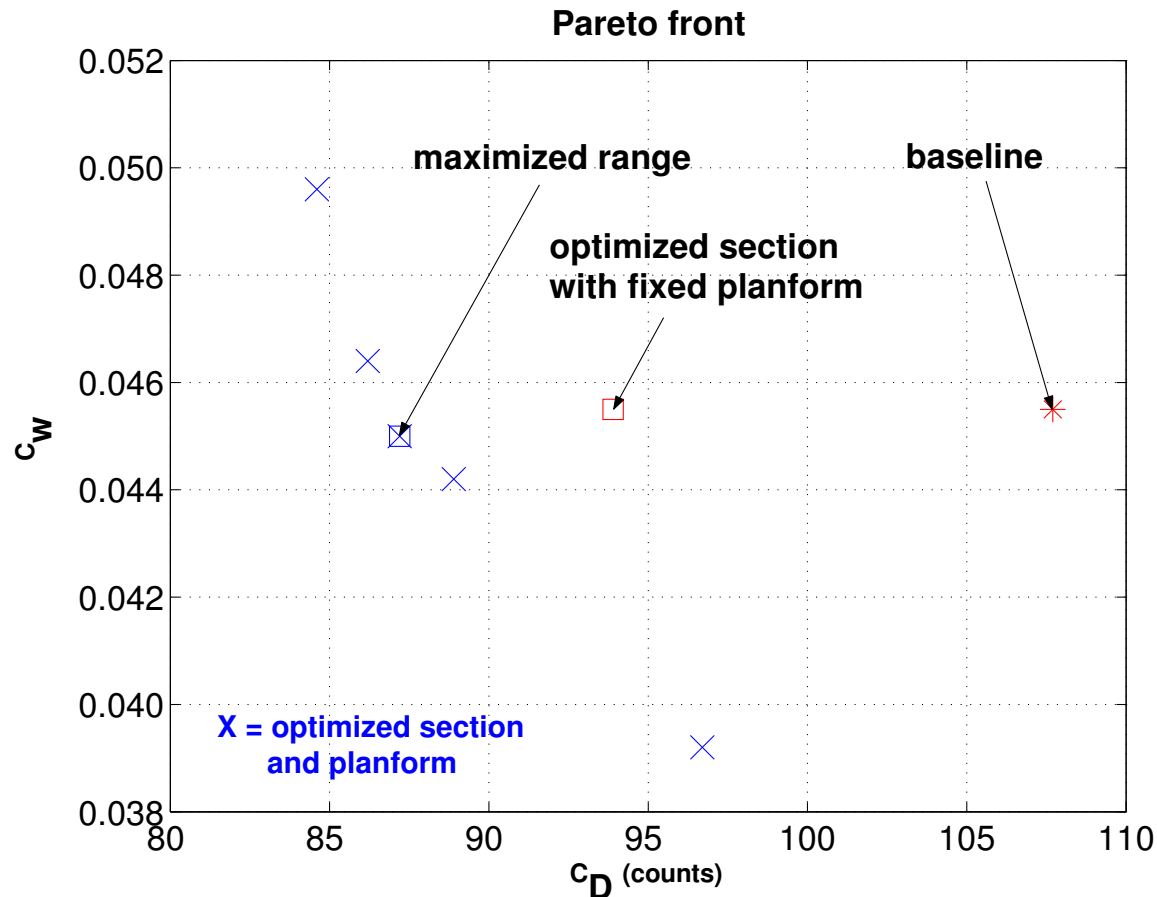
by choosing

$$\alpha = \frac{C_D}{C_{W_2} \log \frac{C_{W_1}}{C_{W_2}}}, \quad (20)$$

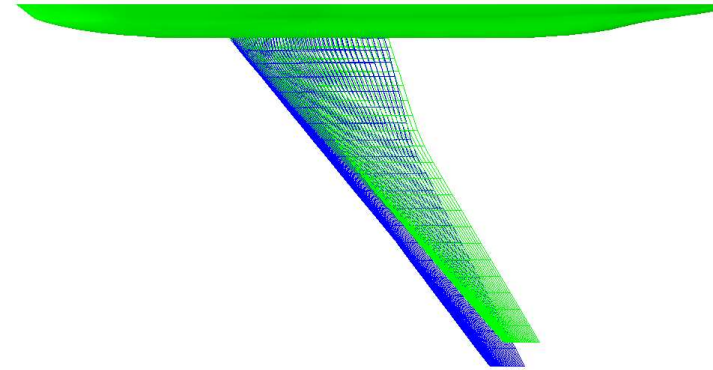
corresponds to **maximizing** the range of the aircraft.

Boeing 747 Euler Planform Results: Pareto Front

Test case: Boeing 747 wing-fuselage and modified geometries at the following flow conditions $M_\infty = 0.87$, $C_L = 0.42$ (fixed), multiple $\frac{\alpha_3}{\alpha_1}$.



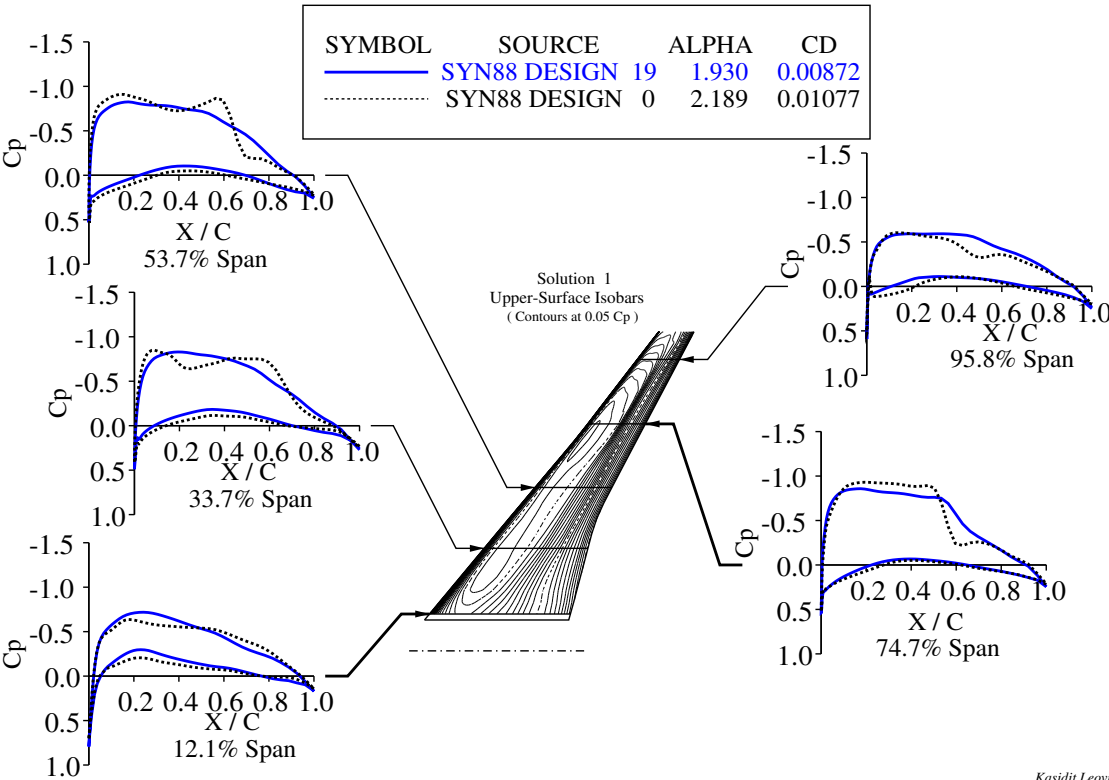
Boeing 747 Euler Planform Results: Sweepback, Span, Chord, and Section Variations to Maximize Range



Baseline geometry —
Optimized geometry —

Geometry	Baseline	Optimized	Variation(%)
Sweep (deg)	42.1	38.8	- 7.8
Span (ft)	212.4	226.7	+ 6.7
C_{root} (ft)	48.1	48.6	+ 1.0
C_{mid} (ft)	30.6	30.8	+ 0.7
C_{tip} (ft)	10.78	10.75	+ 0.3
t_{root} (in)	58.2	62.4	+ 7.2
t_{mid} (in)	23.7	23.8	+ 0.4
t_{tip} (in)	12.98	12.8	- 0.8

SYMBOL	SOURCE	ALPHA	CD
—	SYN88 DESIGN 19	1.930	0.00872
⋯	SYN88 DESIGN 0	2.189	0.01077



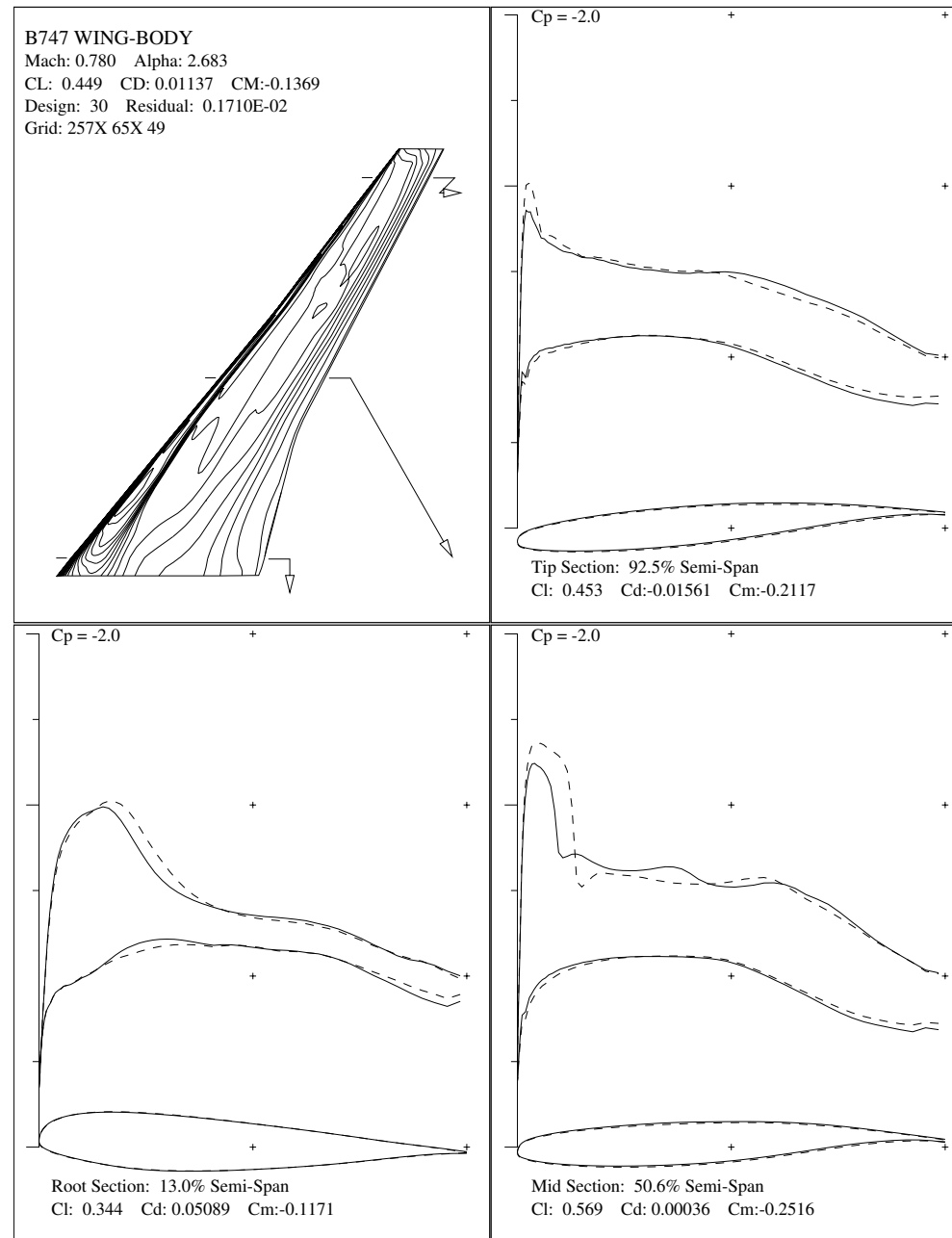
- C_D is reduced from 107.7 drag counts to 87.2 drag counts (19.0%).
- C_W is reduced from 0.0455 (69,970 lbs) to 0.0450 (69,201 lbs) (1.1%).

👉 Super B747

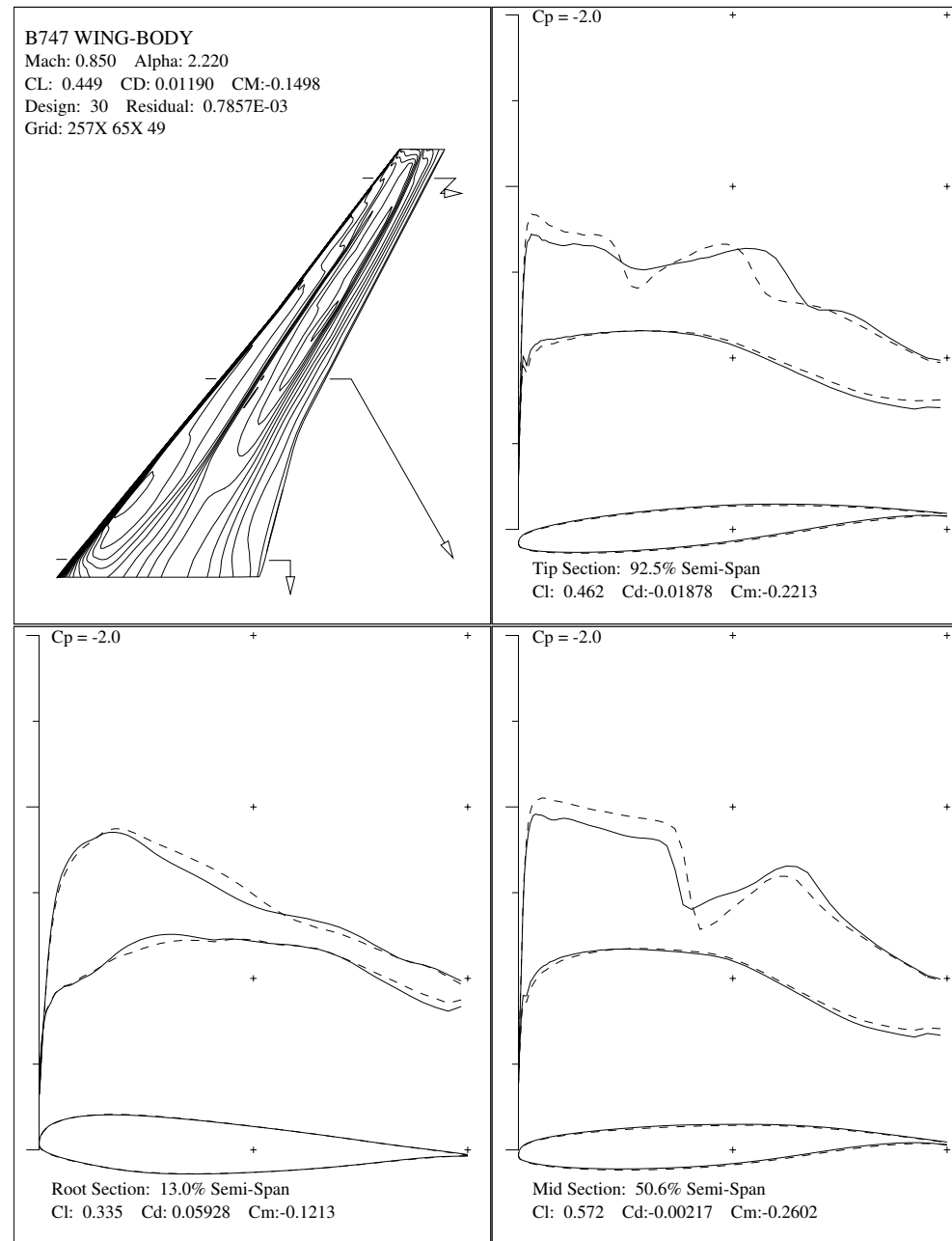


- Design a new wing for the Boeing 747
- Strategy
 - Use the **Boeing 747 fuselage**
 - Use a **new planform** (from the Planform Optimization result)
 - Use **new airfoil section** (AJ airfoils)
 - Optimized for **fixed lift coefficient** at **three Mach numbers:**
.78, .85, and .87

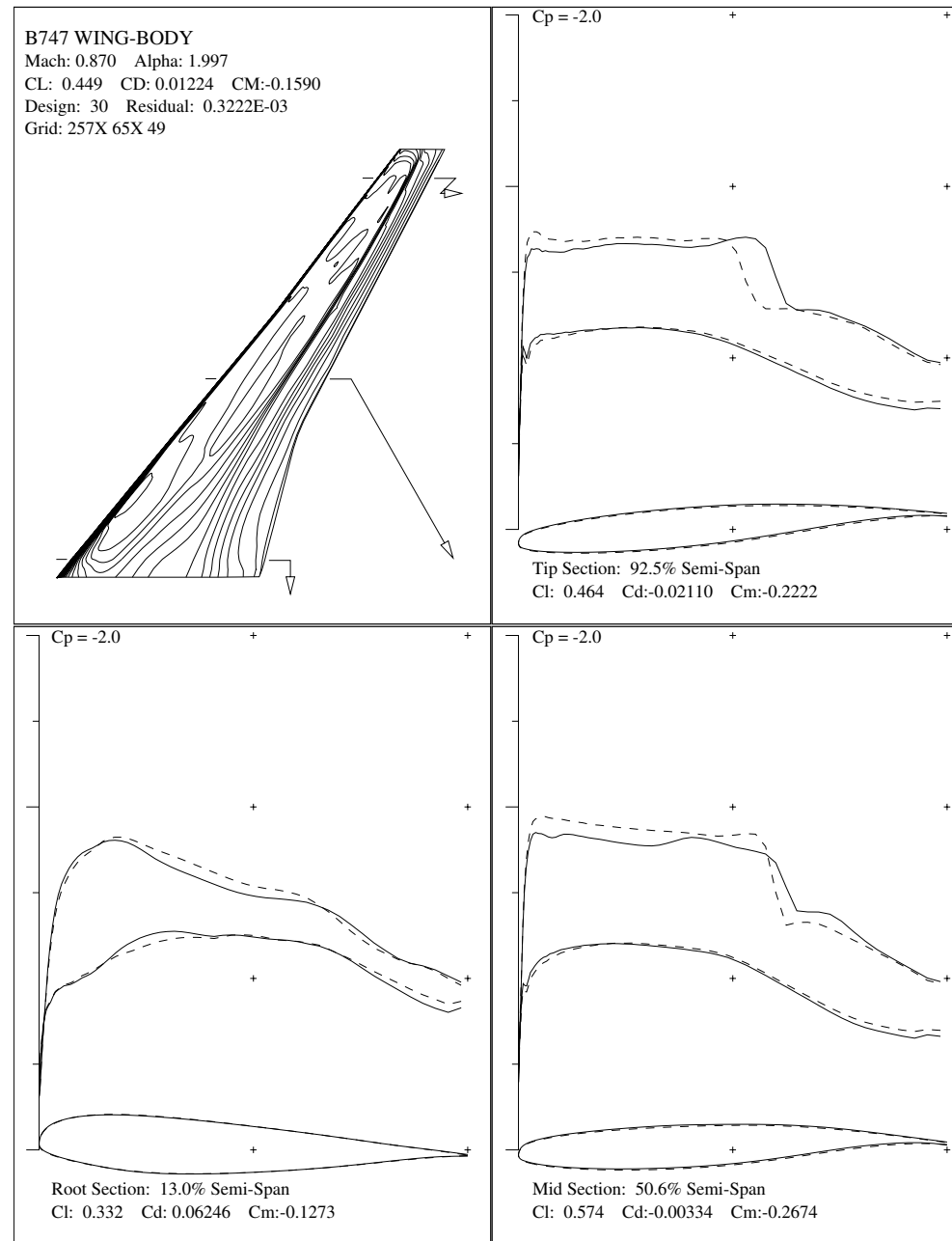
👉 **Super B747 at Mach .78:** (Solid line = redesigned configuration), (Dash line = initial configuration)



👉 **Super B747 at Mach .85:** (Solid line = redesigned configuration), (Dash line = initial configuration)

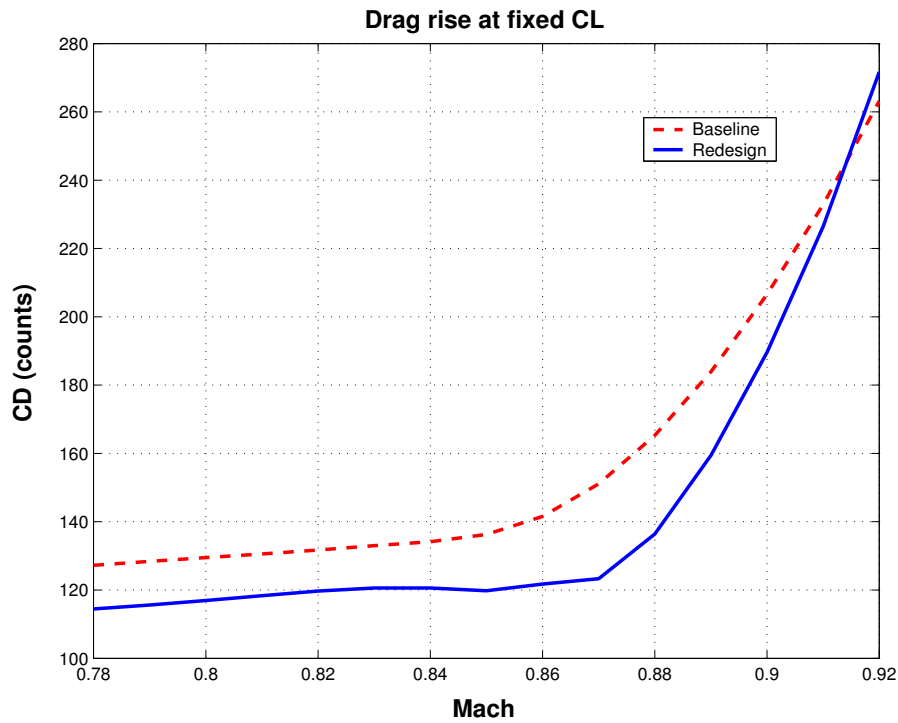


👉 **Super B747 at Mach .87:** (Solid line = redesigned configuration), (Dash line = initial configuration)

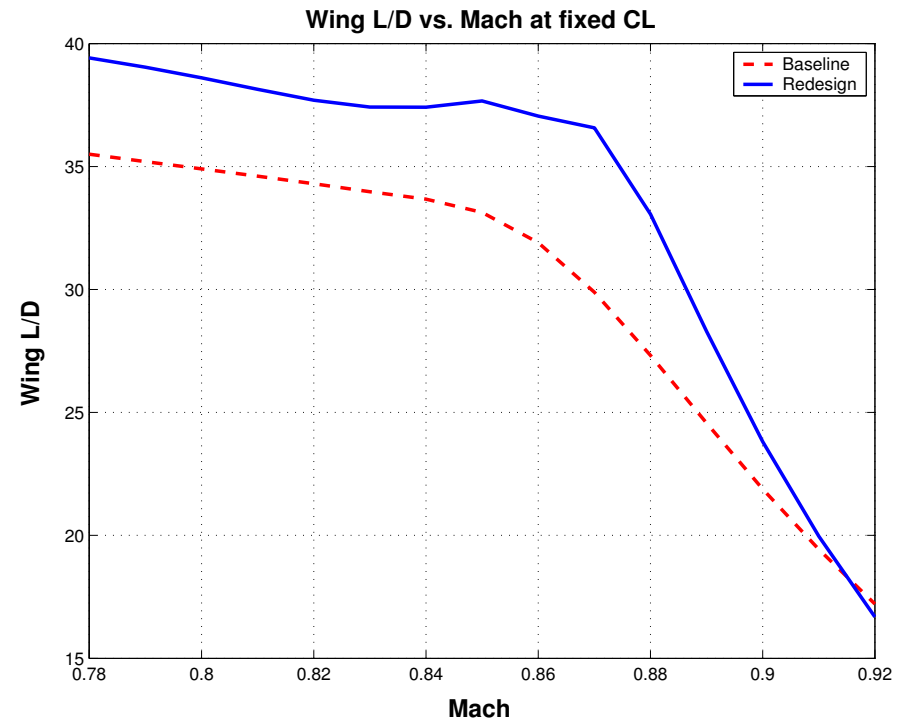


👉 Drag Rise and Wing $\frac{L}{D}$ of Super B747

Drag Rise



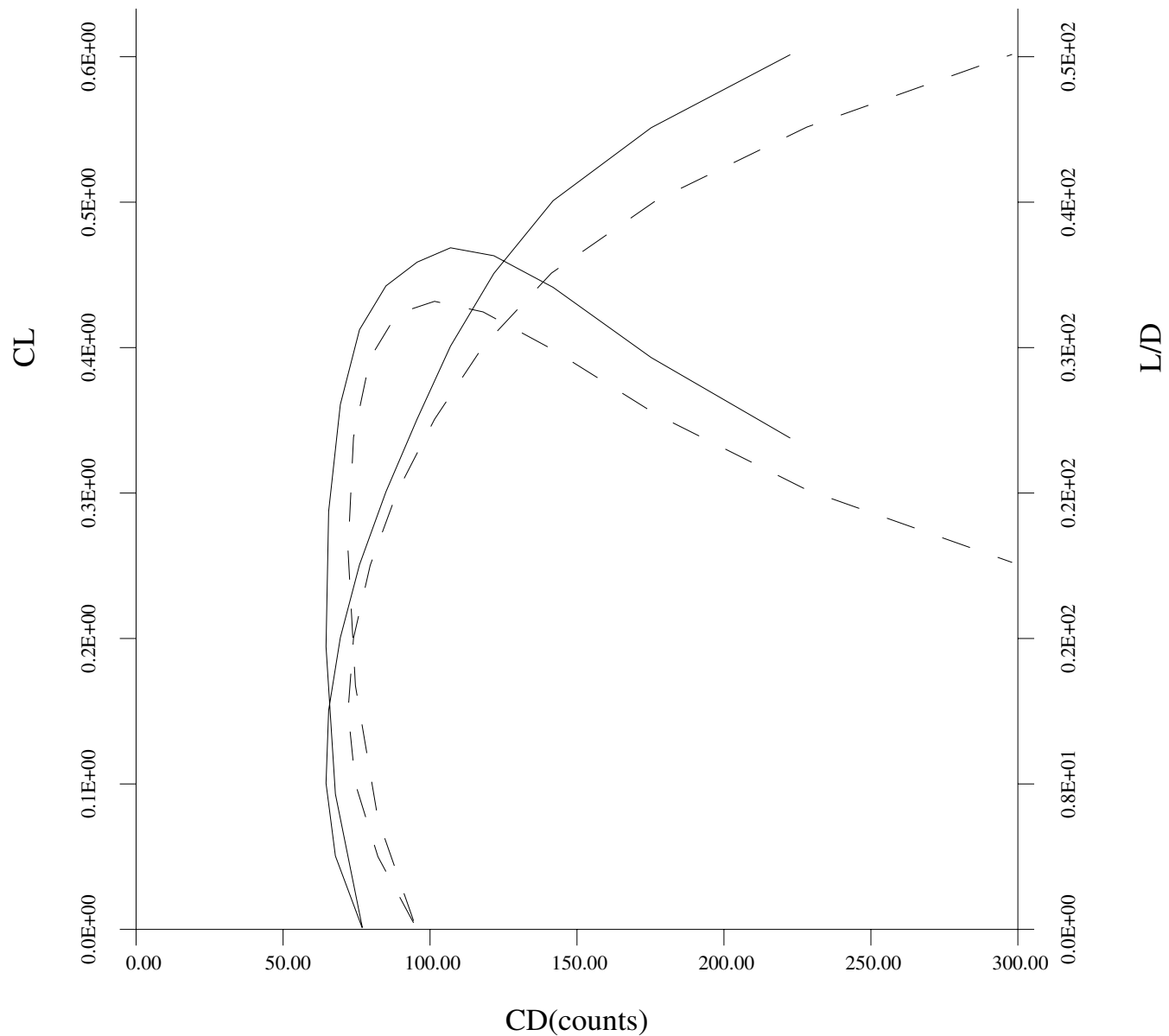
Wing $\frac{L}{D}$



--- : Baseline

— : Redesigned

👉 Drag Polars of Baseline and Super B747 at Mach .86



Solid line = Super B747, Dash line = Baseline B747

☞ Drag Polars of Baseline and Super B747 at Mach .86

Boeing 747		Super B747	
C_L	C_D	C_L	C_D
0.0045	94.3970	0.0009	76.9489
0.0500	82.2739	0.0505	67.8010
0.1000	74.6195	0.1005	64.6147
0.1501	72.1087	0.1506	65.5073
0.2002	73.9661	0.2006	69.4840
0.2503	79.6424	0.2507	76.0041
0.3005	88.7551	0.3008	84.9889
0.3507	101.5293	0.3509	95.6117
0.4009	118.0487	0.4010	106.9625
0.4512	141.2927	0.4510	121.7183
0.5014	177.0959	0.5010	141.8675
0.5516	228.1786	0.5512	175.2569
0.6016	298.0458	0.6014	222.5459

(C_D in counts)

☞ Comparison between Boeing 747 and Super B747

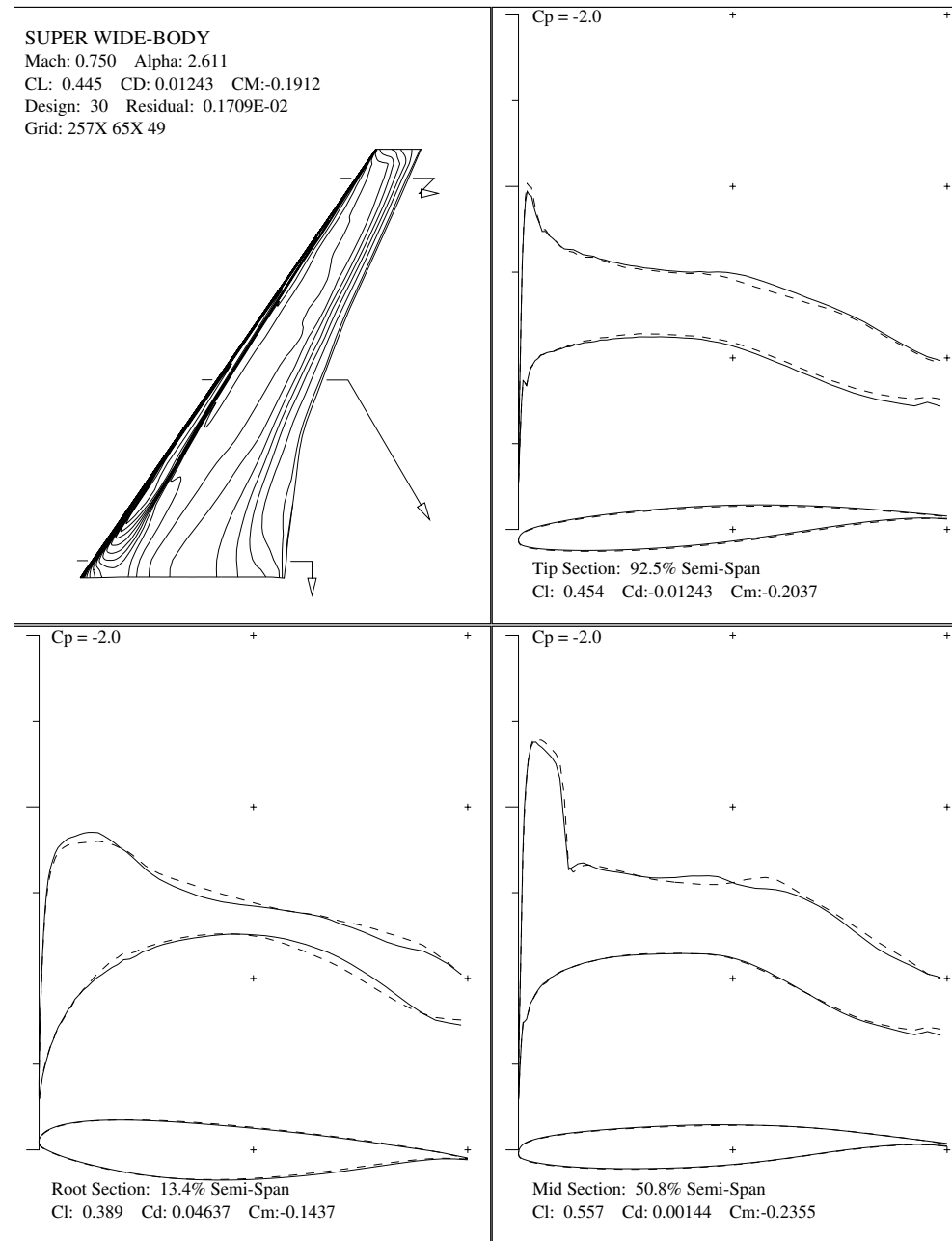
	C_L	C_D counts	C_W counts
Boeing 747	.45	141.3 (107.0 pressure, 34.3 viscous)	499 (82,550 lbs)
Super B747	.50	141.9 (104.8 pressure, 37.1 viscous)	427 (70,620 lbs)

“Same drag at higher C_L ”

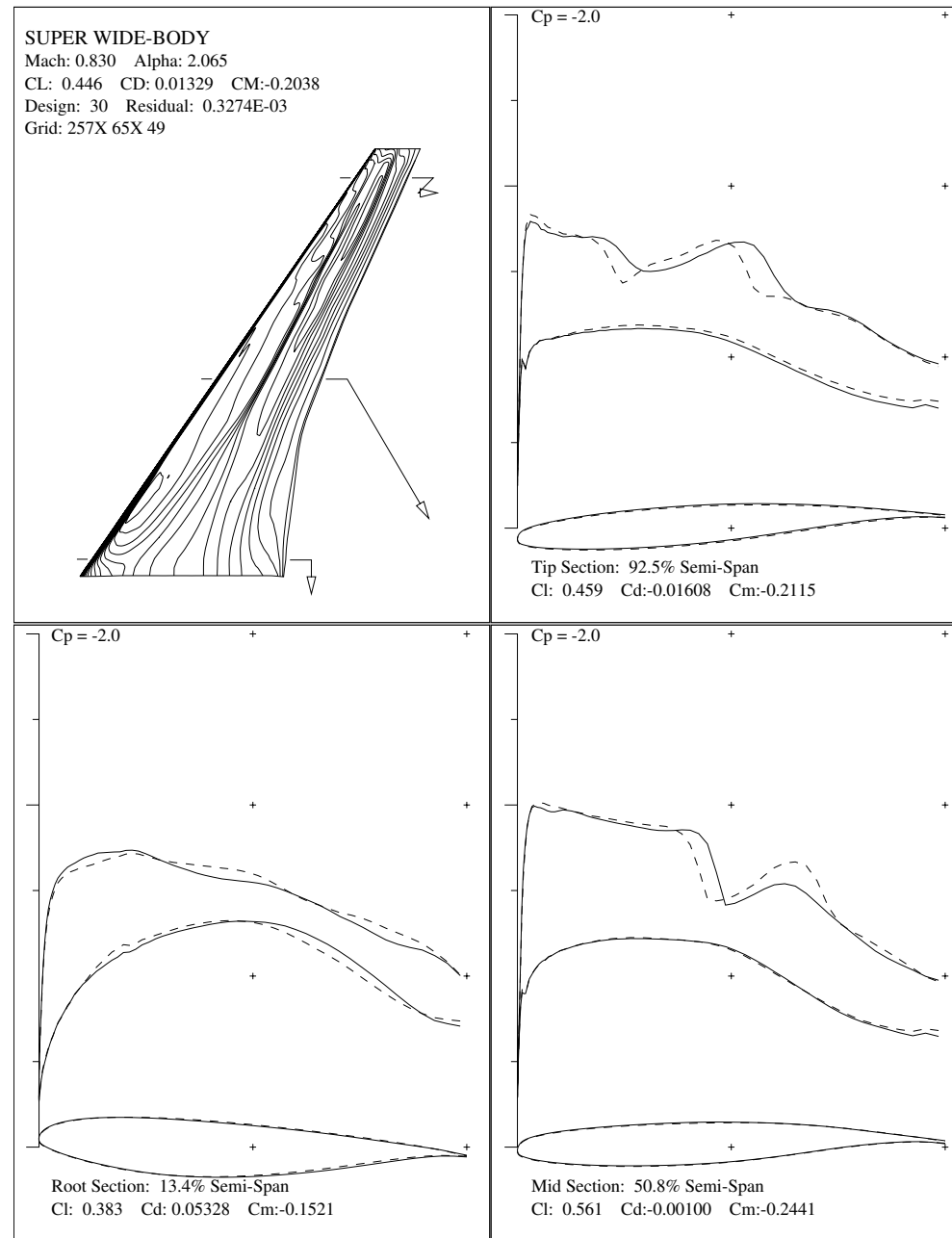
👉 Super Wide-Body



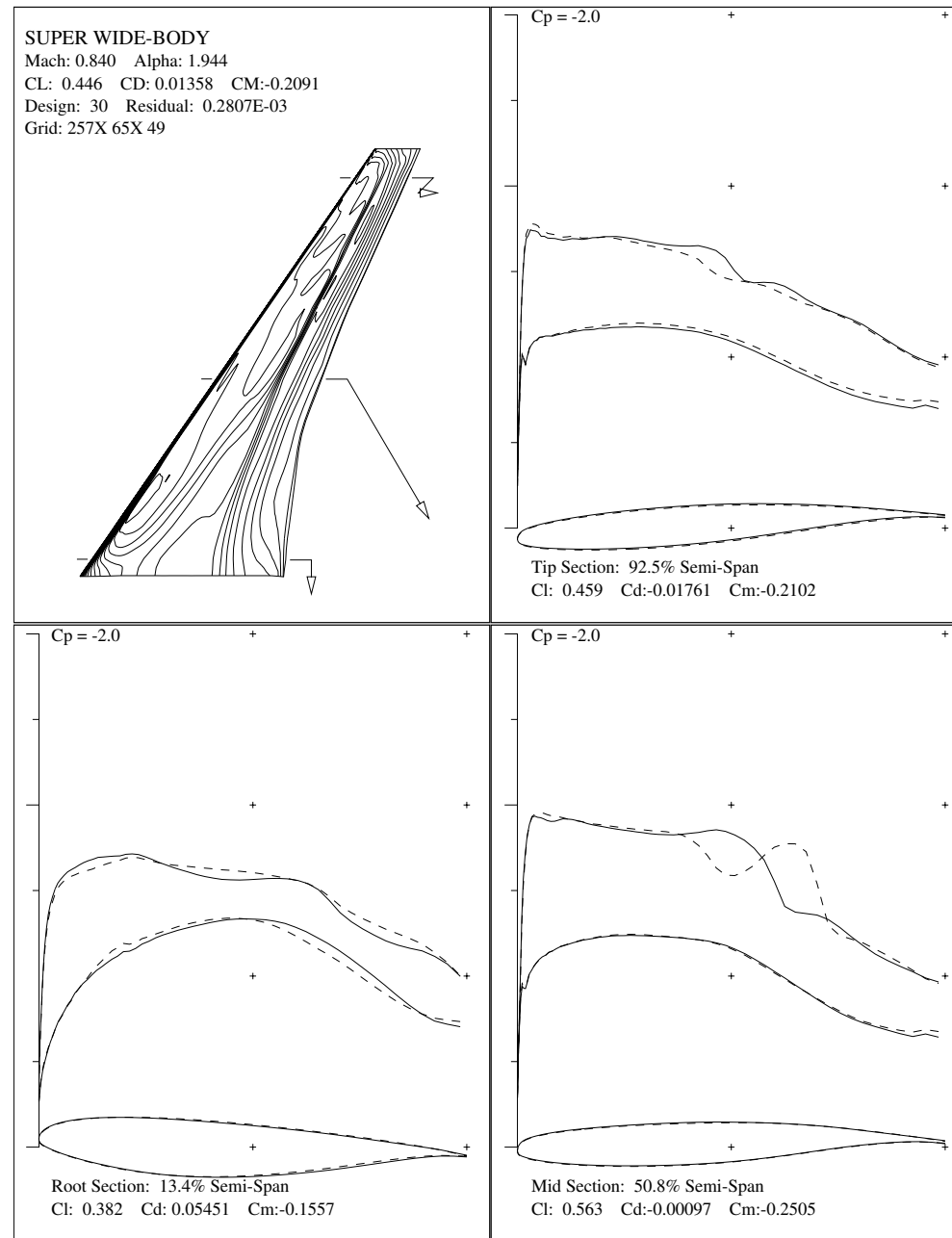
👉 **Super Wide-Body at Mach .75:** (Solid line = redesigned configuration), (Dash line = initial configuration)



👉 **Super Wide-Body at Mach .83:** (Solid line = redesigned configuration), (Dash line = initial configuration)

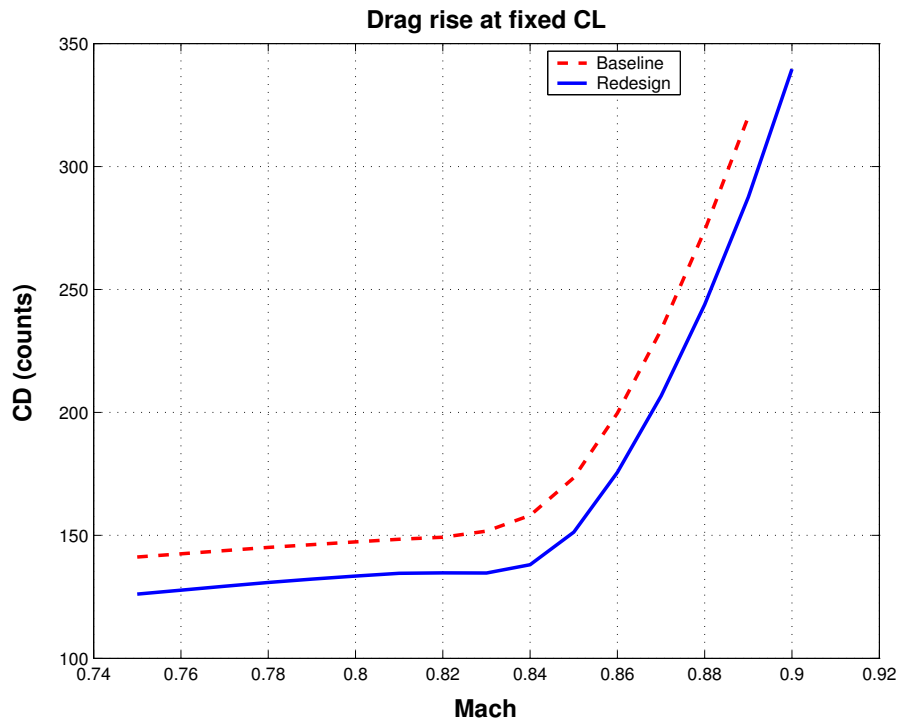


👉 **Super Wide-Body at Mach .84:** (Solid line = redesigned configuration), (Dash line = initial configuration)

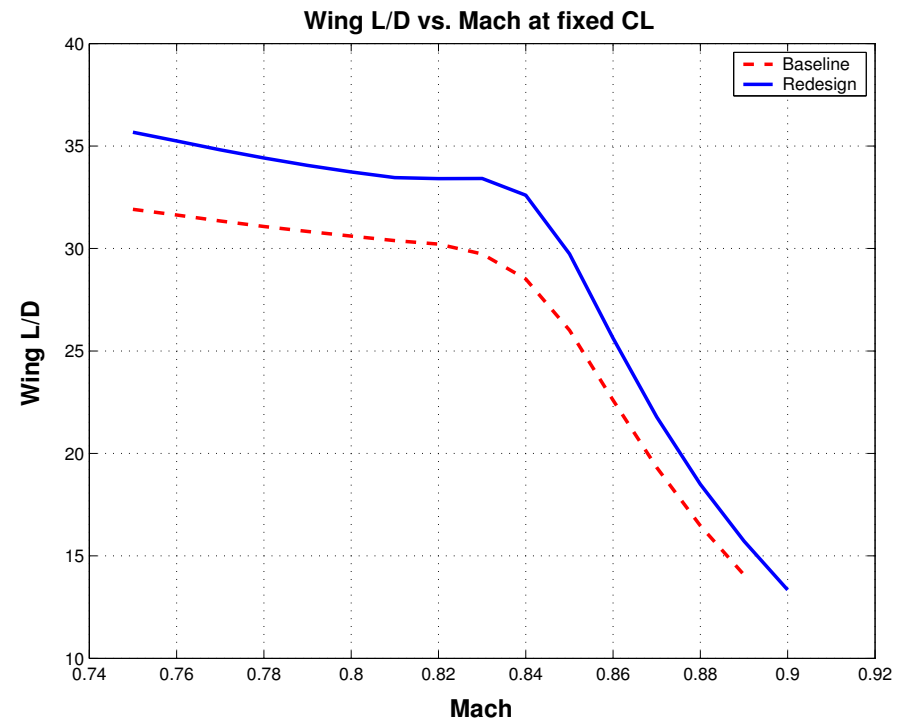


👉 Drag Rise and Wing $\frac{L}{D}$ of Super Wide-Body

Drag Rise



Wing $\frac{L}{D}$



--- : Baseline

— : Redesigned

👉 Shape Optimization of Complete Business Jet Configuration

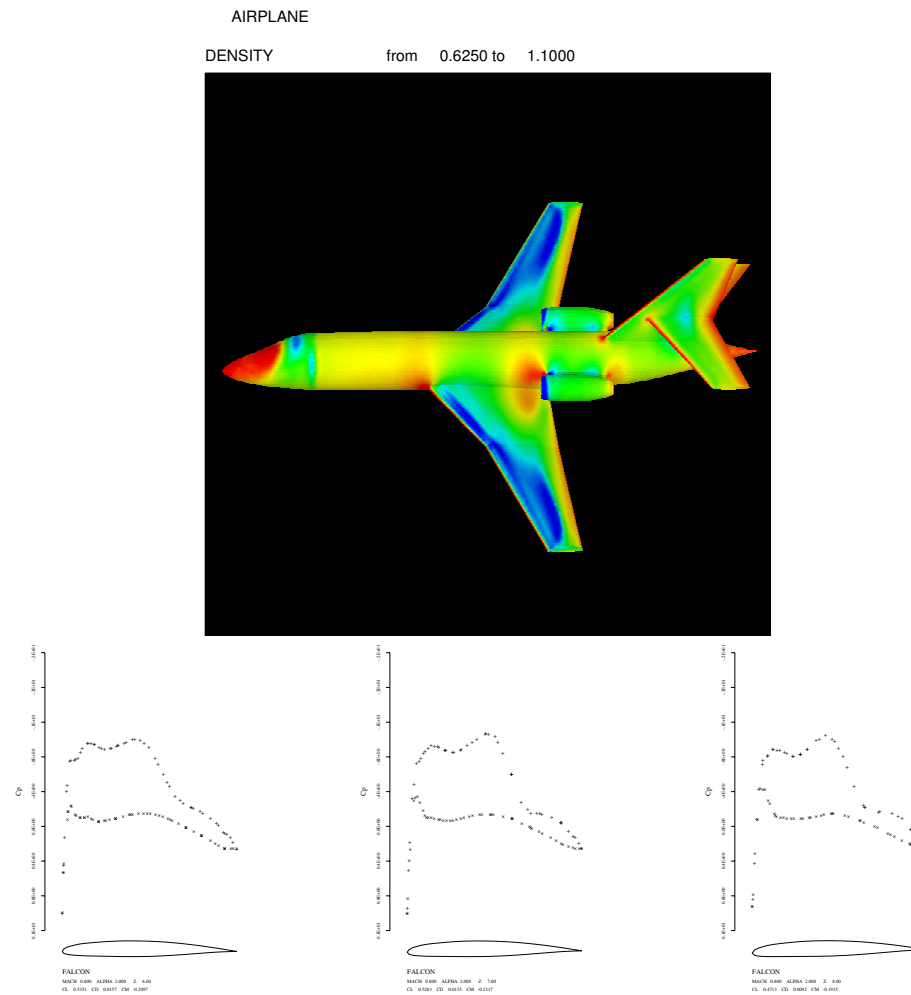
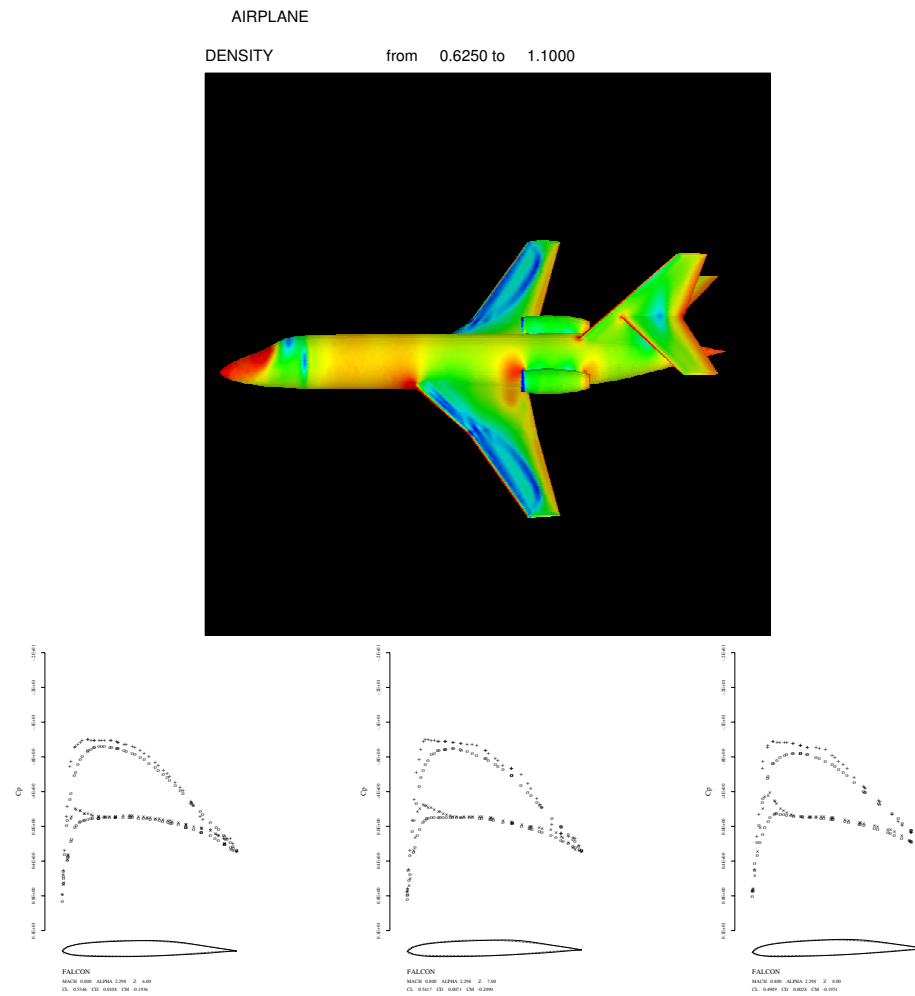


Figure 4: Density contours for a business jet at $M = 0.8$, $\alpha = 2$ and pressure distribution at 66,77,88 % of the wing

👉 Shape Optimization of Complete Business Jet Configuration



Conclusions

- An important conclusion of both the two- and the three-dimensional design studies is that the wing sections needed to reduce shock strength or produce shock-free flow do not need to resemble the familiar flat-topped and aft-loaded super-critical profiles.
- The section of almost any of the aircraft flying today, such as the Boeing 747 or McDonnell-Douglas MD 11, can be adjusted to produce shock-free flow at a chosen design point.

Conclusions

- The accumulated experience of the last decade suggests that most existing aircraft which cruise at transonic speeds are amenable to a drag reduction of the order of 3 to 5 percent, or an increase in the drag rise Mach number of at least .02.
- These improvements can be achieved by very small shape modifications, which are too subtle to allow their determination by trial and error methods.
- When larger scale modifications such as planform variations or new wing sections are allowed, larger gains in the range of 5-10 percent are attainable.

Conclusions

- The potential economic benefits are substantial, considering the fuel costs of the entire airline fleet.
- Moreover, if one were to take full advantage of the increase in the lift to drag ratio during the design process, a smaller aircraft could be designed to perform the same task, with consequent further cost reductions.
- It seems inevitable that some method of this type will provide a basis for aerodynamic designs of the future.